Available online at www.sciencedirect.com
SCIENCE DIRECT®
Journal of Organometallic Chemistry 691 (2006) 2902–2908
Journal of Organometallic Chemistry
www.elsevier.com/locate/jorganchem

Phonon dispersion in poly(dimethylsilane)

Ruchi Agarwal, Poonam Tandon *, Vishwambhar Dayal Gupta

Physics Department, Lucknow University, University Road, Lucknow 226007, Uttar Pradesh, India

Received 27 April 2005; received in revised form 22 February 2006; accepted 24 February 2006
Available online 3 March 2006

Abstract

In the present communication we report normal modes and their dispersion in polydimethylsilane (PDMS) $[–Si(CH_3)_2–]_n$ using Urey–Bradley force field, which in addition to valence force field accounts for the non-bonded interactions in the *gem* and *cis* configurations and tension terms. The partially deuterated PDMS (PDMS-d_3), i.e., $(SiCH_3CD_3)_n$ and fully deuterated PDMS (PDMS-d_6), i.e., $(SiCD_3CD_3)_n$ are also studied to check the assignments and validity of the force field. Dispersion curves show two interesting features: (1) a divergence of dispersion curves following repulsion of species belonging to the same symmetry; (2) crossing between the two modes. In addition, heat capacity as a function of temperature via density-of-states is evaluated and some of the modes left unassigned by the earlier workers have been assigned.

Keywords: Poly(dimethylsilane); Phonon dispersion; Density-of states; Heat capacity; Infrared spectra; Raman spectra

1. Introduction

Polysilanes are a class of polymers, which contain only silicon (Si) atoms in the backbone with organic substituents. They are interesting because of their attractive spectroscopic and semiconducting properties [1,2], photoluminescence, piezochromism, thermochromism [3,4], etc. In recent years interest is focused on electronic and optical properties which are dominated by σ-delocalization on electrons along the main chain. Their structures and conformational properties have been experimentally determined [3,5,6] using empirical force field, semiempirical and ab initio quantum chemical approaches [7–10].

To understand the basic properties of polysilanes, polydimethylsilane (PDMS) $[–Si(CH_3)_2–]_n$ is the simplest representative of the class of such polymers. It is of great interest as the first member of dialkyl substituted Si backbone polymers. PDMS was formed by the reaction of dimethyldichlorosilane monomer with molten sodium metal dispersed in octane. Damewood and West [7] using full relaxation empirical force field methods found that the all *gauche (GG)* conformations should be the lowest in energy for PDMS, with *anti gauche (AG)* and all *anti (AA)* slightly higher [11]. Here, *A* and *G* stand for *anti* and *gauche* as proposed by West [12] and co-workers [13] for the *trans* and *gauche* states having torsional angles of 180° and 60°, respectively. Welsh and Johnson [14] employed molecular mechanics methods with full, partial, or no relaxation of internal degrees of freedom. The full relaxation calculations showed a preference for all *gauche* conformations (in agreement with Ref. [7]), no relaxation yielded *AG* lowest in energy, *AA* only very slightly higher, and *GG* substantially higher (ca. 4 kcal/mol); partial relaxation gave intermediate results. However, more recent studies [10,14] have utilized molecular orbital calculations and concluded that the *anti* state is preferred over *gauche* by 0.6–1.1 kcal/mol. Mintmire [9] utilizing a first principal approach of a linear combination of atomic orbital local density function, found that the smallest band gap for PDMS is obtained for an all *anti* conformation (2.84 eV) and that this increases by ca. 2 eV as the Si backbone is rotated to an all *gauche* structure. The X-ray diffraction studies of Furukawa [15] also support planar backbone

* Corresponding author. Tel.: +91 5222782653.
E-mail address: poonam_tandon@hotmail.com (P. Tandon).

0022-328X/$ - see front matter © 2006 Elsevier B.V. All rights reserved.
doi:10.1016/j.jorganchem.2006.02.032

conformation of PDMS with a monoclinic unit cell with $a = 0.745$, $b = 0.724$, $c = 0.389$ nm and $\gamma = 67.1°$. PDMS undergoes two weak thermal transitions at 160 and 220 °C. First, transition involves preservation of the *anti* conformation and adoption of orthorhombic packing on a metrically hexagonal lattice. The second thermal transition involves additionally some conformational and orientational disordering [11]. From electron diffraction analysis of PDMS [11], it adopts an *anti* conformation. In our calculations we also adopt the planar zigzag *anti* conformation.

Vibrational spectroscopy, being very sensitive to conformational changes, is a suitable tool to characterize the oriented films of PDMS. The infrared (IR) absorption, Raman spectra and inelastic neutron scattering from the polymeric systems are very complex and cannot be unraveled without full knowledge of the dispersion curves. The evaluation of the normal modes of a polymeric system is in general an order of magnitude more difficult than molecular systems. However, the advent of lasers and fast computers has greatly eased this problem. The physical properties of a polymer are strongly influenced by the conformation of the polymer. Vibrational spectroscopy, besides providing information about different conformational states, plays an important role in an understanding of the dynamical behaviour of polymer chains. Normal mode analysis helps in precise assignment and identification of spectral features. The presence of regions of high density-of-states, which appear in all techniques and play an important role in thermodynamical behaviour, is also dependent on the profile of the dispersion curves.

Vibrational studies of PDMS have been reported by many workers [16–20] using IR and Raman spectroscopic methods. Phonon dispersion curves of polysilane $[–SiH_2–]_n$ have been reported by Vora et al. [21]. However, to the best of our knowledge no such detailed studies have been reported on PDMS. In the present communication we report normal modes and their dispersion in PDMS using Urey–Bradley force field, which in addition to valence force field accounts for the non-bonded interactions in the *gem* and *cis* configuration and tension terms. The partially deuterated PDMS (PDMS-d_3), i.e., $(SiCH_3CD_3)_n$ and fully deuterated PDMS (PDMS-d_6), i.e., $(SiCD_3CD_3)_n$ are also studied to check the assignments and validity of the force field. In addition, heat capacity via density-of-states is also determined.

2. Theory

2.1. Calculation of normal mode frequencies

Normal mode calculation for a polymeric chain was carried out using Wilson's GF matrix method [22] as modified by Higgs [23] for an infinite polymeric chain. The vibrational secular equation to be solved is

$$|G(\delta)F(\delta) - \lambda(\delta)I| = 0 \quad 0 \leqslant \delta \leqslant \pi \tag{1}$$

where δ is the phase difference between the modes of adjacent chemical units, $G(\delta)$ is the inverse kinetic energy matrix and $F(\delta)$ is the force field matrix for a certain phase value. The wavenumber $\bar{\nu}_i(\delta)$ in cm^{-1} are related to eigenvalues by $\lambda_i(\delta) = 4\pi^2c^2[\bar{\nu}_i(\delta)]^2$.

A plot of $\bar{\nu}_i(\delta)$ versus δ gives the dispersion curve for the ith mode. The use of the type of force field is generally a matter of one's chemical experience and intuition [24]. In the present work, we have used Urey–Bradley force field [25], as it is more comprehensive than valence force field. The Urey–Bradley takes into account both bonded and non-bonded interactions as well as internal tensions. Potential energy for this force field can be written as

$$\begin{aligned} V = &\sum_{m,j,k} K'_{j,k} r^{(m)}_{j,k} \left(\Delta r^{(m)}_{j,k}\right) + K_{j,k}\left(\Delta r^{(m)}_{j,k}\right)^2 \Big/ 2 \\ &+ \sum_{m,i,j,k} H'_{i,j,k} r^{(m)}_{i,j} r^{(m)}_{j,k} \left(\Delta\alpha^{(m)}_{i,j,k}\right) + H_{i,j,k} r^{(m)}_{j,k} \left(\Delta\alpha^{(m)}_{i,j,k}\right)^2 \Big/ 2 \\ &+ \sum_{m,i,j,k} F'_{i,k} q^{(m)}_{i,k} \left(\Delta q^{(m)}_{i,k}\right) + F_{i,k}\left(\Delta q^{(m)}_{i,k}\right)^2 \Big/ 2 \\ &+ \sum_j K^{\tau}_j \left(\Delta\tau_j\right)^2 + \sum_j K^{\omega}_j \left(\Delta\omega_j\right)^2 \end{aligned} \tag{2}$$

where the symbols have their usual meaning. The primed quantities are introduced as internal tensions. Non-bonded interactions involve attraction and repulsion of atoms due to the overlap of their electron shells. These effects are usually expressed by the 6-exp or 6–12 type potentials. The tension terms are assumed to be all zero.

Recently, spectroscopically effective molecular mechanics model have been used for inter and intra molecular interactions consisting of charges, atomic dipoles and Vander Waals (non-bonded) interactions [26].

The force constants, including those for the interaction of first and third non-bonded atoms, which give the "best fit", are given in Table 1 and have been obtained by least squares fitting. In order to obtain the "best fit" with the observed wavenumbers the following procedure is adopted.

Force constants were initially transferred from the molecules having similar groups placed in the similar environment. Initially the force constants corresponding to the Si group are transferred from cyclic silane Si_6Me_{12} [27] and for CH_3 group are transferred from β poly(L-alanine) $(–CO–C_\alpha H–CH_3–NH–)_n$ [28]. Thus, starting with the approximate F matrix F_0 and observed frequencies λ_{obs} (related through a constant), one can solve the secular matrix equation:

$$GF_0L_0 = L_0\lambda_0 \tag{3}$$

Let $\Delta\lambda_i = \lambda_{i_{obs}} - \lambda_{i_0}$ in the above equation. It can be shown that in the direct order of approximation

$$\Delta\lambda = J\Delta F \tag{4}$$

where J is computed from L_0. We wish to compute the corrections to F_0 so that the errors $\overline{\Delta\lambda}$ are minimized. We used the theory of least squares and calculate

Table 1
Internal coordinates and Urey–Bradley force constants (mdyn/Å)

Internal coordinates	Force constants
ν(C1–H)	4.224
ν(C2–H)	4.224
ν(Si–C1)	1.495
ν(Si–C2)	1.495
ν(Si–Si)	1.240
ϕ(H–C1–H)	0.371 (0.275)
ϕ(H–C2–H)	0.371 (0.275)
ϕ(C1–Si–C2)	0.360 (0.100)
ϕ(Si–C1–H)	0.191 (0.300)
ϕ(Si–C2–H)	0.191 (0.300)
ϕ(Si–Si–C1)	0.169 (0.250)
ϕ(Si–Si–C2)	0.169 (0.250)
ϕ(Si–Si–Si)	0.050 (0.020)
τ(Si–Si)	0.042
τ(Si–C1)	0.005
τ(Si–C2)	0.005
Off diagonal interaction	
ϕ(Si–C1–H) − ϕ(Si–C2–H)	0.090

Note: ν, ϕ and τ denote stretch, angle bend, and torsion, respectively. Non-bonded interactions are given in parentheses.

$$J'P\overline{\Delta\lambda} = (J'PJ)\overline{\Delta F} \tag{5}$$

where P is the weighting matrix and J' is the transposition of J. The solution of this equation is obtained by inverting $J'PJ$ to give

$$\overline{\Delta F} = (J'PJ)^{-1}J'P\overline{\Delta\lambda}. \tag{6}$$

If the number of frequencies is greater than the number of F matrix elements, the matrix $J'PJ$ should be non-singular and be obtain the corrections ΔF, which will minimize the sum of the weighted squares of the residuals. This minimum sum provides the "best fit". If the corrections ΔF are fairly large, the linear relation between force constant and frequency term in the matrix equation (3) breaks down. In such a situation, further refinement using higher order terms in the Taylor's series expansion of $\Delta\lambda_i$ is needed. King et al. [29] developed this procedure.

2.2. Calculation of specific heat

Dispersion curves can be used to calculate the specific heat of a polymeric system. For a one-dimensional system the density-of-states function or the frequency distribution function expresses the way energy is distributed among the various branches of normal modes in the crystal, is calculated from the relation

$$g(\nu) = \sum[(\partial\nu_j/\partial\delta)^{-1}]_{\nu j(\delta)=\nu j}. \tag{7}$$

The sum is over all the branches j. Considering a solid as an assembly of harmonic oscillators, the frequency distribution $g(\nu)$ is equivalent to a partition function. The constant volume heat capacity can be calculated using Debye's relation

$$C_v = \sum g(\nu_j)KN_A(h\nu_j/KT)^2 \times [\exp(h\nu_j/KT)/\{\exp((h\nu_j/KT)-1)\}^2] \tag{8}$$

with $\int g(\nu_i)\,d\nu_j = 1$.

The constant-volume heat capacity C_v, given by above equation, can be converted into constant-pressure heat capacity C_p using the Nernst–Lindemann approximation [30]

$$C_p - C_v = 3RA_0(C_p^2 T/C_v T_m^0) \tag{9}$$

where A_0 is a constant often of a universal value $[3.9\times10^{-3}$ (K mol)/J] and T_m^0 is the estimated equilibrium melting temperature, which is taken to be 660 K [16].

3. Results and discussion

PDMS, with all *anti* conformation, having 9 atoms in a chemical repeat unit (Fig. 1) gives rise to 27 dispersion curves. The frequencies of vibrations are calculated at phase difference values from 0 to π at intervals of 0.05π. The calculated frequencies at $\delta = 0$ and π are optically active. As explained in the theory, the force constants corresponding to the Si group are transferred from cyclic silane Si_6Me_{12} [27] and for CH_3 group are transferred from β poly(L-alanine) $(–CO–C_\alpha H–CH_3–NH–)_n$ [28] and then modified to give the "best fit" to the observed spectra of Leites et al. [17] and Shimomura et al. [19] (Table 1). We have not only used the diagonal force constants but also the off-diagonal force constants. The off-diagonal interactions are also given in Table 1. Urey–Bradley force field takes into account the bonded as well as non-bonded interactions between the *tetra* (1:4) and *geminal* (1:3) atoms as well. The dispersion curves are given in Fig. 2(a) for the modes below 600 cm^{-1}, since the modes above this are non-dispersive. The lower two dispersion curves correspond to four acoustic modes two at $\delta = 0$ and two at $\delta = \pi$. The assignments have been made on the basis of potential energy distribution (PED), band shape, band intensity and appearance/disappearance of modes in similar molecules placed in similar environment. The best matched frequencies along with the PED of the modes are given in Table 2.

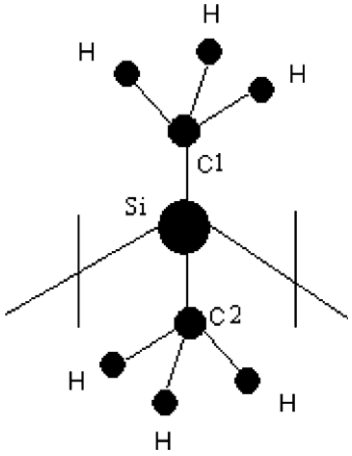

Fig. 1. One chemical repeat unit of PDMS.

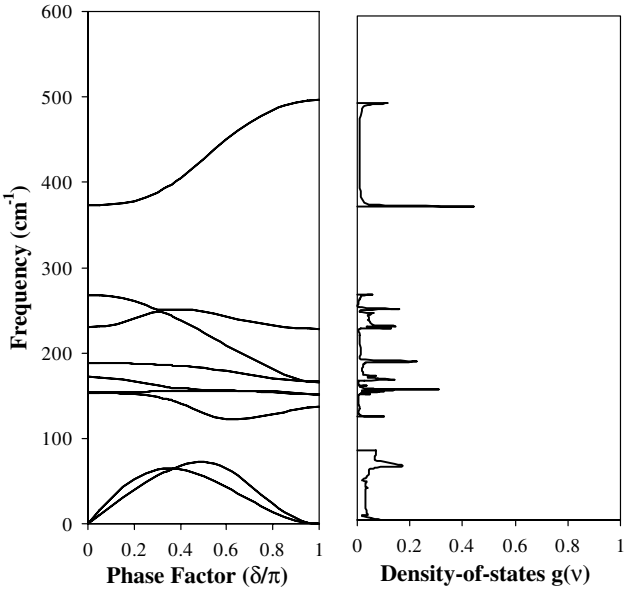

Fig. 2. (a) Dispersion curves of PDMS below 600 cm^{-1}. (b) Density-of-states of PDMS below 600 cm^{-1}.

3.1. Methyl group modes

In PDMS modes above 700 cm^{-1} are associated with the vibrations of two methyl groups attached to the Si atoms in the backbone. The calculated frequencies in the C–H stretching region are in good agreement with the observed bands in PDMS.

The region from 1200 to 1410 cm^{-1} contains asymmetric and symmetric deformation modes of the methyl groups. The calculated frequencies in this region fit well with the observed spectra. The 830–700 cm^{-1} region is methyl rocking region and the separation of the rocking modes at 832 cm^{-1} (symmetric rocking) and 731 cm^{-1} (antisymmetric rocking) in the IR spectra and at 846 cm^{-1} (symmetric rocking) and 746 cm^{-1} (antisymmetric rocking) in the Raman spectra is due to the interaction between the two methyl groups bonded to the same silicon atom [19]. Since our force field does not account for the interactions between the two-methyl groups hence an additional off-diagonal coupling interaction between ϕ(Si–C1–H) and ϕ(Si–C2–H) was taken into consideration (Table 1). All the methyl group modes are well localized and non-dispersive.

Normal mode calculations for deuterated samples are of great importance in checking the correctness of assignments and validity of the force field. Observed spectra for PDMS-d_3 (partially deuterated), i.e., $(SiCH_3CD_3)_n$ and PDMS-d_6 (fully deuterated), i.e., $(SiCD_3CD_3)_n$ derivatives of PDMS have been reported by Shimomura et al. [20]. Normal mode calculations for these two species with the same set of force constants agree with the observed frequency shifts. The H-deuteration of PDMS results in a shift of all those modes that involve the motion of the methyl group. These results are reported in Table 3. This table also contains the (Si–C) stretch modes in PDMS-d_3 and PDMS-d_6 systems. The overall agreement is very good. The divergence in a couple of cases lies within less than 4%. The original and the shifted frequencies obey the product rule [32].

3.2. Other modes

The asymmetric and symmetric Si–C stretching modes are calculated at 669 and 612 cm^{-1}, respectively, at the zone centre. The former is assigned to the observed peak at 668 cm^{-1} in Raman. It disperses to 681 cm^{-1} at zone boundary and assigned to the observed peak at 690/683 cm^{-1} in IR/Raman spectra. The second one at 612 cm^{-1} reaches at 632 cm^{-1} at $\delta = \pi$ and is assigned to the observed IR peak at the same value.

The skeletal stretch mode calculated at 373 cm^{-1} at zone centre shows maximum dispersion (by 123 wave number). This mode is assigned to the observed peak at the same value in the Raman spectra. This mode is highly coupled along the chain and involves coupling of ν(Si–Si) with ϕ(C1–Si–C2) and ϕ(Si–Si–Si). It has little dispersion till $\delta = 0.35\pi$ but beyond it its frequency increases sharply and it becomes a pure mode of Si–Si stretch around 0.55π. Further, a mixing of ϕ(Si–Si–C1) and ϕ(Si–Si–C2) occurs. At the zone boundary the mode reaches at 496 cm^{-1} and is assigned to the observed Raman band at 481 cm^{-1}. In the case of polysilane $(–SiH_2–)_n$, Si–Si stretch was observed at 480 cm^{-1} in Raman spectra [21].

The (Si–Si–C) bending modes are calculated at 268 and 230 cm^{-1} at the zone centre and assigned to the observed peaks at 268 cm^{-1} (Raman) and 216 cm^{-1} (IR), respectively. A prominent feature seen in the dispersion curves of these modes is the repulsion of modes. The repulsion occurs in the neighbourhood of 0.30π. An examination of dispersion and PED of these modes indicates that these modes approach each other, exchange character and then get repelled. This interesting phenomenon of exchange of character may be viewed as a collision in the energy momentum space (ε,p) of two phonons approaching each other and moving apart after exchanging their PED. This characteristic feature arises for the modes belonging to same symmetry species and coupling of corresponding modes. The ϕ(C1–Si–C2) is calculated at 188 cm^{-1} and observed in Raman spectra at the same value. The observed peak at 154 cm^{-1} (IR) is assigned to the τ(Si–C).

The lower two acoustic modes show a crossing at $\delta = 0.365\pi$. At the crossing point the PED of upper mode is ϕ(Si–Si–Si)(37) + ϕ(Si–Si–C2)(25) + ϕ(Si–Si–C1)(25) and of the lower mode is τ(Si–Si)(94). To ascertain whether it is a crossing or repulsion, calculations at very close intervals of $\delta = 0.001\pi$ have been performed and it was found that the modes are crossing over each other. All such points where they cross or repel correspond to some internal symmetry point of the polymer chain in the energy momentum space. It implies two different species existing at the same frequency. They have been called "non-fundamental resonances" [31] and are useful in the interpretation of

Table 2
Normal modes and their dispersion in PDMS

Calculated frequency	Observed frequency		Assignment ($\delta = 0$), PED (%)	Calculated frequency	Observed frequency		Assignment ($\delta = \pi$), PED (%)
	IR	Raman			IR	Raman	
2957	2952	2956	ν(C2–H)(51) + ν(C1–H)(49)	2956	2952	2956	ν(C2–H)(51) + ν(C1–H)(49)
2957	2952	2956	ν(C1–H)(51) + ν(C2–H)(49)	2956	2952	2956	ν(C1–H)(51) + ν(C2–H)(49)
2894	2896	2895	ν(C2–H)(50) + ν(C1–H)(49)	2894	2896	2895	ν(C2–H)(50) + ν(C1–H)(50)
2894	2896	2895	ν(C1–H)(51) + ν(C2–H)(49)	2894	2896	2895	ν(C1–H)(51) + ν(C2–H)(49)
2893	2896	2895	ν(C2–H)(50) + ν(C1–H)(49)	2893	2896	2895	ν(C2–H)(51) + ν(C1–H)(49)
2893	2896	2895	ν(C1–H)(50) + ν(C2–H)(50)	2893	2896	2895	ν(C1–H)(50) + ν(C2–H)(50)
1405	1404	1404	ϕ(H–C2–H)(48) + ϕ(H–C1–H)(48)	1407	1404	1404	ϕ(H–C2–H)(48) + ϕ(H–C1–H)(48)
1401	1404	1404	ϕ(H–C1–H)(49) + ϕ(H–C2–H)(48)	1404	1404	1404	ϕ(H–C1–H)(49) + ϕ(H–C2–H)(47)
1400	1404	1404	ϕ(H–C2–H)(49) + ϕ(H–C1–H)(48)	1403	1404	1404	ϕ(H–C2–H)(49) + ϕ(H–C1–H)(47)
1398	1404	1404	ϕ(H–C1–H)(49) + ϕ(H–C2–H)(48)	1401	1404	1404	ϕ(H–C1–H)(49) + ϕ(H–C2–H)(48)
1248	1248	–	ϕ(H–C2–H)(26) + ϕ(H–C1–H)(26) + ϕ(Si–C2–H)(22) + ϕ(Si–C1–H)(22)	1248	1248	–	ϕ(H–C2–H)(26) + ϕ(H–C1–H)(26) + ϕ(Si–C1–H)(22) + ϕ(Si–C2–H)(22)
1204	–	1238	ϕ(H–C1–H)(26) + ϕ(H–C2–H)(26) + ϕ(Si–C1–H)(22) + ϕ(Si–C2–H)(22)	1205	–	1238	ϕ(H–C1–H)(26) + ϕ(H–C2–H)(26) + ϕ(Si–C1–H)(22) + ϕ(Si–C2–H)(22)
832	832	846	ϕ(Si–C1–H)(46) + ϕ(Si–C2–H)(46)	833	832	846	ϕ(Si–C2–H)(46) + ϕ(Si–C1–H)(46)
790	–	–	ϕ(Si–C2–H)(59) + ϕ(Si–C1–H)(33)	791	–	–	ϕ(Si–C1–H)(46) + ϕ(Si–C2–H)(46)
790	–	–	ϕ(Si–C1–H)(58) + ϕ(Si–C2–H)(32)	790	–	–	ϕ(Si–C2–H)(45) + ϕ(Si–C1–H)(45)
732	731	746	ϕ(Si–C2–H)(45) + ϕ(Si–C1–H)(45)	736	731	746	ϕ(Si–C2–H)(43) + ϕ(Si–C1–H)(43)
669		668	ν(Si–C1)(43) + ν(Si–C2)(43)	681	690	683	ν(Si–C1)(46) + ν(Si–C2)(46)
612	–	–	ν(Si–C1)(42) + ν(Si–C2)(42) + ν(Si–Si)(10)	632	632	–	ν(Si–C1)(47) + ν(Si–C2)(47)
373	–	373	ν(Si–Si)(78) + ϕ(C1–Si–C2)(10) + ϕ(Si–Si–Si)(6)	496	–	481	ν(Si–Si)(81) + ϕ(Si–Si–C1)(8) + ϕ(Si–Si–C2)(8)
268		268	ϕ(Si–Si–C1)(49) + ϕ(Si–Si–C2)(49)	228	–	–	ϕ(C1–Si–C2)(74) + ϕ(Si–Si–C1)(10) + ϕ(Si–Si–C2)(10)
230	216	–	ϕ(Si–Si–C1)(48) + ϕ(Si–Si–C2)(48)	166	–	–	ϕ(Si–Si–C1)(36) + ϕ(Si–Si–C2)(36) + τ(Si–C2)(13) + τ(Si–C1)(13)
188	–	188	ϕ(C1–Si–C2)(75) + ϕ(Si–Si–C1)(11) + ϕ(Si–Si–C2)(11)	166	–	–	ϕ(Si–Si–C2)(37) + ϕ(Si–Si–C1)(37) + τ(Si–C1)(12) + τ(Si–C2)(12)
172	–	–	ϕ(Si–Si–C2)(40) + ϕ(Si–Si–C1)(40)	152	154	–	τ(Si–C2)(38) + τ(Si–C1)(38) + ϕ(Si–Si–C1)(12) + ϕ(Si–Si–C2)(12)
154	154	–	τ(Si–C1)(49) + τ(Si–C2)(49)	151	154	–	τ(Si–C1)(37) + τ(Si–C2)(37) + ϕ(Si–Si–C2)(13) + ϕ(Si–Si–C1)(13)
153	154	–	τ(Si–C1)(44) + τ(Si–C2)(44)	137	–	140	τ(Si–Si)(49) + ϕ(Si–Si–C1)(24) + ϕ(Si–Si–C2)(24)

Note: All frequencies are in cm^{-1}. Observed spectra are from Refs. [9,11]. Only dominant potential energy distributions are given.

Table 3
Comparison of modes of PDMS, PDMS-d_3, PDMS-d_6

	PDMS		PDMS-d_3		PDMS-d_6	
	Calculated frequency	Observed frequency	Calculated frequency	Observed frequency	Calculated frequency	Observed frequency
CH_3 asymmetric stretch	2957	2952^{ir}, 2956^{r}	2957	2951^{ir}		
CH_3 symmetric stretch	2893, 2894	2895^{r}, 2896^{ir}	2893	2895^{ir}		
CD_3 asymmetric stretch			2143, 2142	2210^{ir}	2141, 2142, 2143	2209^{ir}
CD_3 symmetric stretch			2113	2112^{ir}	2113	2112^{ir}
CH_3 asymmetric deformation	1405, 1401, 1400, 1398	$1404^{ir,r}$	1404, 1403	1414^{ir}		
CH_3 symmetric deformation	1248	1248^{ir}	1228	1246^{ir}		
	1204	1238^{r}				
CD_3 asymmetric deformation			1018, 1017	1030^{ir}	1019	1034^{ir}
					1018, 1017, 1016	1028^{ir}
CD_3 symmetric deformation			947	980^{ir}	962	981^{ir}
					927	–
CH_3 rock	832	832^{ir}, 846^{r}	793	795^{ir}		
	790	–	786	746^{ir}		
	732	731^{ir}, 746^{r}				
CD_3 rock			587	584^{ir}	589	581^{ir}
			569	569^{ir}		
Si–C stretch	681	690^{ir}, 683^{r}	673	700^{ir}	660	680^{ir}
	669	668^{r}	605	600^{ir}	552	567^{ir}
	632	632^{ir}				

Note: All frequencies are in cm^{-1}. Observed spectra for PDMS-d_3, PDMS-d_6 are from Ref. [12].

the spectra and interactions involved. When the approaching modes belong to different symmetry species then the two modes can crossover. These crossings are permissible if there is a mirror plane of symmetry [32]. Since we have considered an isolated chain, hence the discussion on dispersion curves; especially the symmetry relation is confined to one-dimensional system with C_{2v} point group symmetry at phase angle 0. The eigenvectors of all modes with a particular value of δ away from the zone centre or zone boundary form a restricted set of the complete set of distortion of the molecule and the molecule now behave as if it no longer has the symmetry of the line group. The only symmetry operation, which may leave any number of such a set unchanged, is reflection in a mirror plane containing the chain axis. In other words modes corresponding to a given $\delta(\neq 0$ or $\pi)$ will belong to one of two symmetry species, depending on whether they are symmetric or antisymmetric with respect to the mirror plane. Therefore, no two dispersion curves both of which belong to the same one of these two species can cross because this would imply the existence of two modes of vibrations with the same symmetry species and same frequency.

Dispersion curves provide knowledge of the degree of coupling and information concerning the dependence of the frequency of a given mode on the sequence length of ordered conformations. In addition, the evaluation of dispersion curves for a three-dimensional (3D) system is somewhat involved both in terms of dimensions and large number of interactions; it is not easy to solve it without first solving the problem for a linear isolated chain. It has been generally observed that, the intramolecular interactions (covalent, non-bonded) are generally stronger than the intermolecular interactions (hydrogen bonding and non-bonded). Crystal field only leads to splitting near the zone centre and zone boundary. The basic profile of the dispersion curves remains more or less unaltered. Thus, the study of phonon dispersion in polymeric system continues to be an important one. They are also useful in calculating the density of vibrational states, which in turn can be used for obtaining thermodynamic properties such as specific heat, entropy, enthalpy and free energy.

4. Frequency distribution and heat capacity

From the dispersion curves frequency distribution function has been obtained and plotted in Fig. 2b. The observed frequencies compare well with these peak positions. The peaks in the dispersion curves correspond to the regions of high density-of-states. This information of density-of-states is used for the calculation of heat capacity as a function of temperature as explained in the theory.

Experimental values of heat capacity for PDMS are given in ATHAS Data Bank only in the temperature range between 160 and 200 K [33]. Their analysis is based on separation of the vibrational spectrum into group and skeletal vibrations. The former are taken from computations fitted to IR and Raman data and the later by using the two parameter Tarasov model and fitting to low temperature heat capacities. This approach is good when full dispersion curves are not available. However, it has its own limitations especially when the modes are strongly coupled. We have calculated heat capacity of PDMS as a function of temperature, from the dispersion curves via density-of-states (Fig. 3). Theoretical details have already been given. There is a very good agreement between calculated values of the specific heat and the experimental measurements.

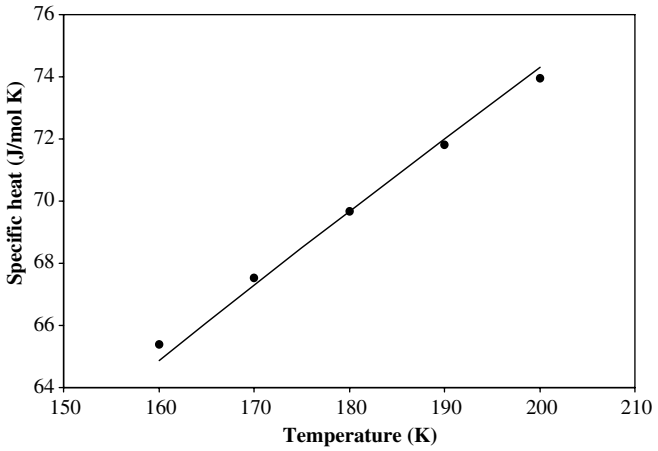

Fig. 3. Variation of heat capacity of PDMS as a function of temperature. Solid line represents the theoretical values and (•) represents the experimental data.

The discrepancy at the low temperature could arise for two reasons, one the neglect of interchain interactions at low temperature and the other because of force field being temperature independent. The former leads to low frequency lattice modes that are not included in the present model and the heat capacity is sensitive to these. The evaluation of lattice modes is not only prohibitive dimensionally but even the enormities of interactions are difficult to visualize. As for the later, the temperature dependence of force field is difficult to build in the potential field.

In spite of several limitations involved in the calculation of specific heat the present work does provide good starting point for further basic studies on thermodynamical behaviour of polymers, which go into well-defined conformations.

5. Conclusion

Urey–Bradley force field successfully explains all the characteristic features of dispersion curves such as regions of high density-of-states, crossover and repulsion. In addition, the heat capacity as a function of temperature in the 160–200 K region has been accounted for as compared with the experimental data reported in ATHAS.

Acknowledgement

Financial assistance to R.A. and P.T. from UP Council of Science & Technology, Lucknow is acknowledged.

References

[1] R.G. Kepler, J.M. Ziegler, L.A. Harrah, S.R. Kurtz, Phys. Rev. B 35 (1987) 2818.
[2] M. Stolka, H.J. Yuh, K. McGrane, D.M. Pai, J. Polym. Sci., Part A: Polym. Chem. Ed. 25 (1987) 823.
[3] R.D. Millar, J. Michl, J. Chem. Rev. 89 (1989) 1359.
[4] K. Song, R.D. Millar, J.F. Rabolt, Macromolecules 26 (1993) 3232.
[5] V.R. Mccrary, F. Sette, C.T. Chen, A.J. Lovinger, M.B. Robin, J. Stohr, J.M. Zeigler, J. Chem. Phys. 88 (1988) 5925.
[6] F.C. Schilling, F.A. Bovey, A.J. Lovinger, J.M. Zeigler, Bull. Am. Phys. Soc. 33 (1988) 657.
[7] J.R. Damewood Jr., R. West, Macromolecules 18 (1985) 159.
[8] W.J. Welsh, J.R. Damewood Jr., R. West, Macromolecules 22 (1989) 2947.
[9] J.W. Mintmire, Phys. Rev. B39 (1989) 13350.
[10] C.X. Cui, A. Carpfen, M. Kertesz, Macromolecules 23 (1990) 3302.
[11] A.J. Lovinger, D.D. Davis, F.C. Schilling, F.J. Padden, F.A. Bovey, J.M. Zeigler, Macromolecules 24 (1991) 132–139.
[12] R. West, Chem. Organicsilicon Comp. 3 (2001) 541.
[13] J. Michl, R. West, Acc. Chem. Res. 33 (2000) 821.
[14] W.J. Welsh, W.D. Johnson, Macromolecules 23 (1990) 1881.
[15] S. Furukawa, J. Organomet. Chem. 611 (2000) 36.
[16] J.P. Wesson, T.C. Williams, J. Polym. Sci. Polym. Chem. Ed. 17 (1979) 2833.
[17] L.A. Leites, S.S. Bukalov, T.S. Yadritzeva, M.K. Mokhov, B.A. Antipova, T.M. Frunze, V.V. Dement'ev, Macromolecules 25 (1992) 2991.
[18] M. Shimomura, T. Yatabe, A. Kaito, Y. Tanabe, Macromolecules 30 (1997) 5570.
[19] M. Shimomura, H. Kyotani, A. Kaito, Macromolecules 30 (1997) 7604.
[20] M. Shimomura, N. Tanigaki, A. Kaito, Korea Polym. J. 7 (1) (1999) 6.
[21] P. Vora, S.A. Solin, P. John, Phys. Rev. B 29 (1984) 3423.
[22] E.B. Wilson, J.C. Decius, P.C. Cross, Molecular Vibrations: The Theory of Infrared and Raman Vibrational Spectra, Dover Publications, New York, 1980.
[23] P.W. Higgs, Proc. R. Soc. Lond. A220 (1953) 472.
[24] B. Mannfors, K. Palmo, S. Krimm, J. Mol. Struct. 556 (2000) 1.
[25] H.C. Urey, H.C. Bradley, Phys. Rev. 38 (1931) 1969.
[26] W. Qian, N.G. Mirikin, S. Krimm, Chem. Phys. Lett. 315 (1999) 125.
[27] K. Hassler, Spectrochim. Acta 37A (7) (1981) 541.
[28] R.M. Misra, V. Saxena, P. Tandon, V.D. Gupta, Polym. J. 37 (1) (2005).
[29] W.T. King, I.M. Mills, B.L. Crawford, J. Chem. Phys. 27 (1957) 455.
[30] R. Pan, M. Verma-Nair, B. Wunderlich, J. Therm. Anal. 35 (1989) 955.
[31] S. Rastogi, V.D. Gupta, J. Macromol. Sci. Phys. B34 (1995) 1.
[32] D.I. Bower, W.F. Maddams, The Vibrational Spectroscopy of Polymers, Cambridge University Press, Cambridge, 1989, pp. 154–156.
[33] ATHAS Data Bank Update, University of Tennessee, Knoxville, USA, 1997.